Reconfigurable Intelligent Surfaces in 6G mMIMO NOMA Networks: A Comprehensive Analysis

Original Scientific Paper

Mohamed Hassan
Department of Electrical Engineering,
Omdurman Islamic University, Omdurman, Sudan,
mhbe4321@gmail.com

Khalid Hamid
Department of Electrical Engineering,
Omdurman Islamic University, Omdurman, Sudan,
khalidhamidk9@gmail.com

Rashid A. Saeed*
Department of Computer Engineering, College of Computers and Information Technology,
Taif University, P.O. Box 11099, 21944, Taif, Saudi Arabia,
abdulhaleem@tu.edu.sa

*Corresponding author

Hesham Alhumyani
Department of Computer Engineering, College of Computers and Information Technology,
Taif University, P.O. Box 11099, 21944, Taif, Saudi Arabia,
h.alhumyani@tu.edu.sa

Abdullah Alenizi
Department of Information Technology, College of Computer and Information Sciences,
Majmaah University, Al-Majmaah 11952, Saudi Arabia,
aalenizi@mu.edu.sa

Abstract *– As the features and characteristics of six-generation (6G) connectivity are defined, advanced technologies such as multiple-input, multiple-output (mMIMO), non-orthogonal multiple access (NOMA), and reconfigurable intelligent surfaces (RISs) are becoming more important for many Internets of Things (IoT) uses. This study comprehensively and uniquely investigates the impact of RIS on the effectiveness of NOMA download (DL) mMIMO systems in the IoT environment within the context of the 6G network. This work aims to analyze the impact of including the RIS in the spectral efficiency (SE) and capacity performance of proposed hybrid system-enabled IoT setting device distributions, such as clustered and hotspot configurations. It highlights the ability of RIS to optimize wireless latency communication and throughput, depending on the mobility and density of IoT devices, respectively. The proposed methodologies are assessed through a simulation software application, under unstable channel conditions with varying distances and power locations while accounting for 256-quadrature amplitude modulation (256-QAM), frequency selective Rayleigh fading, and successive interference cancellation (SIC) context inside the 6G network environment. The results indicate that the four IoT groups (50, 100, 150, and 200) achieved capacity improvements of 5.84%, 5.81, 5.78, and 5.8%, and SE increases of 5.759%, 5.755%, 5.753%, and 5.84%, respectively, when utilizing RIS compared to their performance without it. The implementation of RIS yielded latency rate enhancements of 16.44%, 12.24%, 9.75%, and 8.1% across all four IoT groups, respectively, at a mobility speed of 120 Km/h. Each of the four IoT groups had throughput enhancements of 26%, 25.6%, 25.3%, and 25%, respectively, while using RIS within a coverage area of 400 square meters (sqm).*

Keywords: *Internet of Things, SE, massive MIMO (mMIMO), NOMA, RIS*

Received: Received: September 7, 2024; Received in revised form: October 25, 2024; Accepted: October 26, 2024

1. INTRODUCTION

The fifth generation (5G) represented a substantial advancement in network design, incorporating crucial technologies such as network slicing, centralized radio access networks (C-RAN), and improved mobile broadband. It facilitated reduced latency, increased capacity, and enhanced service flexibility with technologies including massive multiple-input multiple-output (mMIMO), beamforming, and edge computing. Nonetheless, sixth-generation (6G) aspires to surpass 5G in architectural design.

5G has yielded significant economic benefits, enabling progress in autonomous vehicles, industrial automation, and smart city development. However, 6G is expected to have a far higher impact, driving digital transformation throughout all sectors.

Numerous individuals assert that the emergence of 6G would herald a new technological epoch defined by the transmission of vast digital data among interconnected devices, humans, and automobiles. This interaction will build a self-sustaining ecosystem based on development and life. This ecosystem will utilise artificial intelligence (AI) to provide novel services.

The Internet of Things (IoT) is fundamentally transforming our way of life. It profoundly modifies human interactions with one another and their surroundings. According to the IoT concept, connections may be established across all entities and individuals [1, 2]. It is projected that by 2025, the number of IoT devices will have surpassed 100 billion, marking an unparalleled surge.

Many believe that the arrival of 6G will begin a new technological age in which interconnected devices, people, and cars will exchange vast quantities of digital data. Through this connection, an ecosystem that is self-sufficient and based on both development and life will be developed. This ecosystem will use artificial intelligence (AI) to provide novel services. The IoT is fundamentally transforming our way of life. It fundamentally reconstructs how individuals engage with one another and with their surroundings. Following the IoT paradigm, it is possible to establish connections between everything and everyone. The proliferation of IoT devices has been experiencing an unparalleled surge, with certain projections indicating that it may surpass 100 billion by the year 2025 [3-7].

Smart applications in many fields, including healthcare, smart cities, and industrial automation, are made possible by the IoT. A network is a collection of interconnected devices capable of direct communication with each other. With billions of devices relying on 6G, the IoT is anticipated to function at a large scale, necessitating low latency, and great reliability. Efficient management of spectrum resources and ensuring robust connectivity are essential for the effective service of a vast number of IoT devices [8].

To achieve the criteria of 6G, including minimal latency, optimal spectral efficiency (SE), feasible data rates, user fairness, and communication with a large number of devices [9], the non-orthogonal multiple access (NOMA) approach has been introduced, as described in [10]. NOMA is a crucial technology in wireless systems that improves spectrum efficiency. In contrast to conventional orthogonal multiple access (OMA) systems, NOMA enables several users to exploit the same frequency band by distinguishing them based on power levels [11]. This facilitates concurrent transmission to many users, enhancing system capacity and ensuring equitable treatment of users, particularly in situations characterized by a dense concentration of IoT devices [12].

The mMIMO means putting a lot of antennas at the base station (BS) so that it can serve a lot of customers at once. This improves SE and coverage. mMIMO is essential in 6G to meet the significant data throughput and low latency demands of IoT applications. It also improves the network's ability to manage the considerable connectivity required by IoT [13]. Recently, researchers have explored NOMA in mMIMO systems to improve spectrum efficiency [14]. A significant step towards better service quality has been the merging of these two technologies, especially when using huge devices in the IoT, as well as addressing two important challenges, including massive connectivity and low latency.

Reconfigurable intelligent surfaces (RISs) are surfaces that are fitted with programmable components capable of reflecting and manipulating electromagnetic waves in a desired way. In 6G, the RIS is strategically implemented to boost signal quality, expand coverage, and optimize the performance of IoT devices by dynamically adjusting the wireless environment.

Different from current solutions, RIS regulates wireless environment behaviour deterministically and programmatically. The majority of RIS implementations use 2D metasurface arrays. Tuning each element's phase shift skill fully changes signal propagation. Communication ancillary technology like amplification and forwarding relays uses more energy than RIS [14]. RIS technology offers a fresh approach to improving NOMA system performance by recreating the wireless environment; hence, we are strongly encouraged to incorporate RIS into NOMA [15]. The study examines the constraints and potential complications of traditional NOMA as user numbers rise, attributed to successive interference cancellation (SIC) at each user. Space-time block code-assisted NOMA (STBC-CNOMA) needs fewer SICs than traditional NOMA [16].

They thought about a communication setting where all users are the same, with NOMA users clustered together. In their studies, the writers of [17-19] looked at the issues with resource management in multi-cell MIMO networks. For instance, to maximize the users' total capacity, the writers in [20-22] offered a less-than-ideal plan. Their findings demonstrated that NOMA systems can still achieve considerable gains in user capacity when inferior approaches are used.

Moreover, [23] investigated the benefits of RIS in a parasitic radio (SR) system. The authors devised passive and active RIS and BS beamforming to reduce BS transmission power. These designs were based on two constraints: the rate constraint for core communication and the signal-to-interference-plus-noise ratio (SINR) for decoding backscattered signals.

The system models in references examined networks with users using a single antenna throughout the network, therefore constraining the productivity of IoT devices. For instance, in order to maximize the users' total capacity, the writers in [24- 27] offered a less-than-ideal plan. Their findings demonstrated that NOMA systems can still achieve considerable gains in user capacity when inferior approaches are used.

Moreover, [28] investigated the benefits of RIS in a parasitic radio (SR) system. The authors devised passive and active RIS and BS beamforming to reduce BS transmission power. These designs were based on two constraints: the rate constraint for core communication and the signal-to-interference-plus-noise ratio (SINR) for decoding backscattered signals.

The system models in references [29, 30] examined networks with users using a single antenna throughout the network, therefore constraining the productivity of IoT devices.

The majority of the prior work on IRS-enabled NOMA systems was based on the premise of a perfectly stable channel, which is not feasible for real-world situations. However, further investigations are still needed to improve the performance of RIS and NOMA. This work mainly highlights the following contributions:

- This study examines the effects of implementing the RIS in a mMIMO DL NOMA-enabled IoT environment. By implementing RIS, the research demonstrates substantial enhancements in both capacity and SE across different IoT user distributions, showcasing the capability of RIS to optimize wireless communication systems in 6G networks.
- The work investigates the efficiency of NOMA systems throughout various distributions of IoT devices, including clustered and hotspot setups. Incorporating user distribution patterns into the simulation enhances its realism by accurately representing the impact on system performance and exploring the system's scalability and strategies for efficiently combining mMIMO systems with RIS to enhance the overall performance of NOMA systems in IoT networks.
- The paper looks at how well IoT devices handle latency at different mobility speeds with and without RIS. It gives useful information about how well RIS works in different situations by looking at unstable channel conditions, Rayleigh fading, and SIC. We aim to enhance the system's realism, emulate the actual environment, adhere to design constraints, and boost its performance.

The following is the structured rest of the article. A concise review of the pertinent literature is presented in Section 2. The mathematical formulation procedures and the network model specifics are detailed in Section 3. The suggested system parameters, findings, and discussions are presented in Section 4. Section 5 offers final thoughts and recommendations for further research.

2. RELATED WORKS

The study in [31] provides a clear and thorough explanation of RIS technology, addressing its rationale, applications, and locations of usage, while also discussing the challenges and corresponding solutions. However, the case study was extremely inadequate in terms of the number of users. [32] provided an extensive overview of RIS systems, emphasizing their operational principles, performance assessment, development, design, and interaction with other new technologies. Nevertheless, the issues confronting RIS technology during congestion or mobility and their effects on performance were not recognized.

[33] examines NOMA utilizing RIS, concentrating on enhancing power allocation for each user and bandwidth configuration in RIS, while guaranteeing compliance with minimum rate, latency, and reliability standards. The numerical findings indicate that the suggested strategy attains an acceptable rate. The system is predicated only on optimizing power allocation, which presents a constraint as the cumulative power allocations total one and are distributed at varying rates dependent on the number of users and their respective locations. The developed NOMA system with RIS partitioning improves SE by increasing user fairness and ergodic rate [34]. The balanced sum rate, outage probability, and user fairness performance of the proposed system beat the benchmark systems. The primary concept is around the partitioning of RIS; yet, the system has not been thoroughly examined, particularly concerning significant aspects like interference.

Two successful IRS-based channel estimate algorithms for different channel parameters in a multi-user broadband communication system with orthogonal multiple access (OMA) are proposed in [35]. The findings demonstrate that the suggested channel estimation techniques and training strategies outperform comparator systems. NOMA surpasses OMA since the BS consistently determines the user's position and transmits the appropriate power, hence enhancing the implementation of these approaches and yielding better outcomes. The use of IRS to improve coverage by facilitating communication between the cell edge user device and the base station is examined in [36] for both DL and uplink (UL) NOMA and OMA networks. When compared to complete decoding and forward relay, the findings show that IRS is far better. However, the dimensions and spacing of cells for RIS to accommodate edge users remain undetermined.

For signal cancellation-based RISs in the MIMO NOMA network that supports concurrent users, a novel passive beamforming weight design is offered [37]. According to the findings of the analysis, inter-group interference may be eliminated by using a high number of components. In contrast to the anomalous reflector scenario, the diffuse dispersion scenario requires line-of-sight for the BS-RIS and RIS-user connections, which causes shortcomings in this methodology. The mMIMO BS with RIS powers IoT devices wirelessly and enables multiple data users. The BS's precoding uses dual-band transmission and an instantaneous stable channel, whereas the RIS's passive beamforming uses a progressively moving statistically stable channel. Pilot contamination and channel estimation errors were used to generate closed-form formulae for IoT device information user SE and average power [38]. Nevertheless, the mechanism for the distribution of IoT devices and the sort of network employed remains undetermined. The following Table 1 provides a very simplified and comparative analysis of our work with previous literature, with a brief explanation of our contributions.

Table 1. Comparison with previous literature and contributions to the paper

Author's Name	IOT	RIS	NOMA	mMIMO	Device Mobility	6G
C. Pan (2021)	-	✓	-	-	-	-
Y. Liu (2021)	✓	✓	✓	✓	-	✓
Z. Ding (2023)	-	✓	✓	-	-	-
E. Basar (2022)	-	✓	✓	-	-	-
B. Zheng (2020)	-	✓	-	-	-	-
Y. Cheng (2021)	-	✓	✓	-	-	-
T. Hou (2020)	✓	✓	✓	-	-	-
H. Q. Ngo (2024)	✓	✓	✓	✓	-	-
This work	✓	✓	✓	✓	✓	✓

3. SYSTEM MODELS

Assuming the IoT setup using mMIMO and downlink (DL) NOMA, we will determine the system's primary components and how they interact with each other, as shown in Figs. 1 and 2.

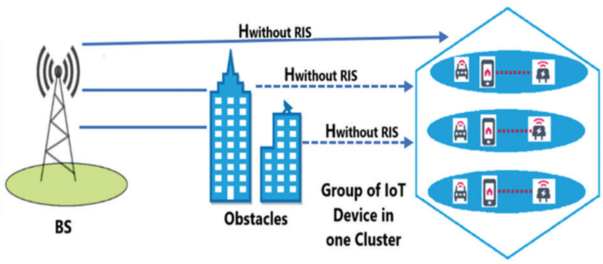

Fig. 1. IoT mMIMO DL NOMA system without RIS technology

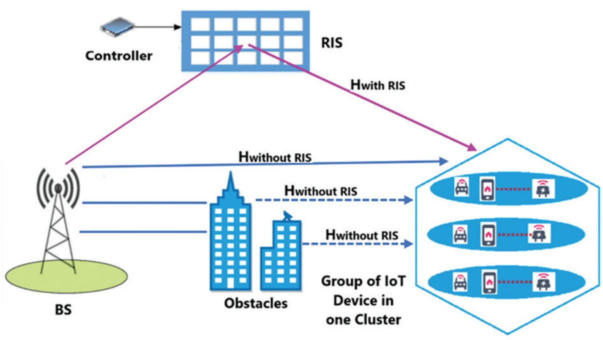

Fig. 2. IoT mMIMO DL NOMA system with RIS scheme

The BS has an array of 128 x 128 mMIMO antennas. By distinguishing between users' power levels, the BS enables numerous IoT devices to share the same frequency band through NOMA signal transmission, and each IoT device has an antenna [39]. In the given case, the clustered distribution model involves grouping devices into clusters and the Rayleigh fading channel model is utilized to characterize the wireless channel between the BS and the IoT devices. The channel model incorporates path loss, antenna gains, RIS enhancement, and mobility effects. Frequently, this assumption accurately represents the actual signal issues and challenges that devices encounter in specific regions.

Under the same prior assumptions, the proposal system engages with the RIS in the second scenario. In this configuration, the base station employs the identical mMIMO architecture as previously to engage with several IoT devices. The channel matrix H represents the mMIMO system that consists of N_{Tx} broadcast antennas and N_{Rx_r} receive antennas, $H \in C^{N_{Rx} \times N_{Tx}}$). The channel matrix H between the BS and an IoT device in the mMIMO system is denoted as:

$$H = \frac{L_p G}{N_{Rx} \times N_{Tx}} \tag{1}$$

In this equation, L_p represents large-scale path loss, whereas G represents small-scale Rayleigh fading channel coefficients. It can be expressed as:

$G \sim CN(0,1)$, where $CN(0,1)$denotes a complex Gaussian distribution characterised by a mean of zero and a variance of one.

The BS concurrently accommodates several IoT devices utilizing the NOMA concept. In NOMA, numerous users utilize the same frequency and temporal resources, differentiated by their power levels [40]. The BS assigns varying power levels to customers according to their channel conditions, guaranteeing that those with superior channels receive reduced power, while those with inferior channels receive more power. This is articulated as follows: For K users or devices, the power assigned to the k-th user or device is represented as P_k, with $\sum_{k=1}^{K} Pk = P_{total}$, where P_{total} signifies the total available power.

In the given case, the clustered distribution model involves grouping devices into clusters with unstable channel conditions. Frequently, this assumption accurately represents the actual signal issues and challenges that devices encounter in specific regions.

let x represent the transmit signal vector from the BS.

$$x = Ws \tag{2}$$

For each user K, the symbol vector is represented by $s \in C^{K \times 1}$. W, which is a precoding matrix applied at the BS, is defined as $W \in C^{N_t \times K}$. Channel matrices in mMIMO systems with no RIS. Adjustments can be made to the channel gain in a clustered distribution to accurately represent the increased signal intensity resulting from the proximity of users inside clusters [41].

$$G_{base} = G_{base\_factor} \times G_{cluster\_adjust} \tag{3}$$

G_{base} is total system gain, including base gain factor and clustering modifications. Without clustering effects, G_{base_factor} is the system or antenna setup's inherent gain. Such as antenna efficiency, transmission power, etc. $G_{cluster\_adjust}$ multiplicative modification to base gain. This adjustment factors in gain increases from beamforming, geographical clustering, and user clustering to optimize signal strength [42].

$$G_{base}=G_{base\_factor}\times G_{hotspot\_adjust} \quad (4)$$

$G_{hotspot\_adjust}$ is multiply adjustments for enhanced signal gain in hotspot locations. Regions with a higher user concentration or stronger signal focus may have higher gain due to localized optimizations such beamforming, power allocation, or signal upgrades [43].

The channel matrix H_{withis} improved by the RIS matrix R upon its introduction,

$$H_{with\ RIS}=H_{without\ RIS}\cdot R \quad (5)$$

where H_{with} is the channel matrix when the RIS or another transformation (beamforming, phase-shifting, etc.) is used. The channel matrix $H_{without}$ represents the direct channel between transmitter and receiver, without any modification. R is a transformation matrix used by the RIS to enhance or improve channel conditions by applying phase shifts or adjustments to incoming signals.

The diagonal matrix R, which represents RIS, contains phase shifts denoted as,

$$R=diag(e^{j\phi_1},e^{j\phi_2},\ldots,e^{j\phi_{NRIS}}) \quad (6)$$

The number of RIS elements is represented by N_{RIS}. The phase shift of the *i-th* RIS is denoted by ϕ_i. The complex phase shift is referred to as the equation $e^{j\phi_i}$). For the channel gain without RIS,

$$Gain_{eff}=Gain_{base} \quad (7)$$

For the channel gain with RIS, the effective channel gain is,

$$Gain_{eff}=Gain_{base}\times RIS_{enhancement} \quad (8)$$

where $RIS_{enhancement}$ Enhancement factor provided by RIS. Examine the intermediary channel connecting the BS and the user devices. The signal y_k received by user K precisely represented as [44],

$$y_k = h_k^H W s + n_k \quad (9)$$

The user k's channel vector is represented as $h_k \in C^{N_t\times 1}$. The additive white Gaussian noise (AWGN) with variance $\sigma_n^{\ 2}$ is denoted by $n_k \sim CN(0, \sigma_n^{\ 2})$. $h_k^{\ H}$ the Hermitian (conjugate transpose) of the h_k. In the case of RIS, the channel vector h_k is increased by the channel information signal RIS. Consider the channel $G \in C^{N_{RIS}\times N_t}$ connecting the BS to RIS, and the channel $v_k \in C^{N_{RIS}\times 1}$ connecting the RIS to user k. The effective channel h_k with RIS can be expressed as [45],

$$h_k = v_k^H \Theta G + h_{direct,k} \quad (10)$$

This is the RIS phase shift matrix: Θ=diag($\theta_1, \theta_2, \ldots, \theta_{N_{RIS}}$), where the *i-th* RIS element introduces a phase shift, denoted as θ_i. Without utilising the RIS, the direct connection from the BS to user k is represented as channel $h_{direct,k}$. The signal strength received by user k without RIS is [46],

$$P_{no\ RIS,k} = |h_k^H W_k|^2 P_{tx} \quad (11)$$

The received signal power changes in the RIS scenario to,

$$P_{with\ RIS,k} = \left|(v_k^H \Theta G + h_{direct,k})^H W_k\right|^2 P_{tx} \quad (12)$$

where P_{tx} is the transmit power. The user k's SNR is calculated as,

$$SNR_{no\ RIS,k} = \frac{P_{tx}\cdot\left|h_k^H W_k\right|^2}{\sigma_n^2} \quad (13)$$

$$\mathrm{SNR}_{\mathrm{with\ RIS,k}} = \frac{P_{tx}\cdot\left|(v_k^H \Theta G + h_{direct,k})^H W_k\right|^2}{\sigma_n^2} \quad (14)$$

user's allotted transmit power is denoted as P_{tx}. By applying the Shannon-Hartley theorem, we may determine user k's capacity C_k,

$$C_k = \frac{BW}{K}\cdot \log_2(1+SNR_k) \quad (15)$$

The total bandwidth is denoted by BW. K is the number of users. The capacity normalized by the bandwidth is the SE_k for user k,

$$\mathrm{SE}_k = \frac{1}{K}\cdot \log_2(1+SNR_k) \quad (16)$$

The Capacity and SE of the System Overall with and Without RIS,

$$C_{no\ RIS,k} = \frac{BW}{K}\cdot \log_2\left(1+\frac{\left|P_{tx}\cdot h_k^H W_k\right|^2}{\sigma_n^2}\right) \quad (17)$$

$$SE_{no\ RIS,k} = \frac{1}{K}\cdot \log_2\left(1+\frac{\left|P_{tx}\cdot h_k^H W_k\right|^2}{\sigma_n^2}\right) \quad (18)$$

$$C_{with\ RIS,k} = \frac{BW}{K}\cdot \log_2\left(1+\frac{P_{tx}\cdot\left|(v_k^H \Theta G + h_{direct,k})^H W_k\right|^2}{\sigma_n^2}\right) \quad (19)$$

$$SE_{with\ RIS,k} = \frac{1}{K}\cdot \log_2\left(1+\frac{P_{tx}\cdot\left|(v_k^H \Theta G + h_{direct,k})^H W_k\right|^2}{\sigma_n^2}\right) \quad (20)$$

Device mobility, network load, and channel conditions all affect communication system latency. This model is used for broad analysis,

$$L = L_{base} + D_{mob} + D_{load} \quad (21)$$

The total network delay (L) comprises base latency, mobility delays, and network load delays.

L_{base} refers to the system's intrinsic latency under ideal conditions, excluding mobility and network load considerations. D_{mob}: The delay during user or device movement, determined by speed and distance. D_{load} refers to the delay caused by network traffic. As network congestion or user activity grows, this delay increases. Network load delay, this metric quantifies the influence of the present network load on the delay [47].

$$L_{without\ RIS} = L_{base} + \alpha\cdot M + \beta\cdot N \quad (22)$$

$$L_{with\ RIS} = L_{base} + \alpha\cdot M\cdot R + \beta\cdot N \quad (23)$$

where, M is network users' or devices' speed or mobility, which affects latency owing to handovers and dynamic connection quality. N is network traffic or users, with larger loads causing congestion and delay.

R scales the RIS's latency impact. α is a proportionality constant that affects latency increase with movement. The constant β measures the influence of network load on latency, by scaling congestion's contribution to overall delay.

$$D_{mob} = \gamma\cdot S\cdot d \quad (24)$$

D_{mob} is a Mobility Delay. Speed is S. Distance (D). The mobility delay coefficient is γ.

where, γ is a proportionality constant. S is the speed of the device. D is the distance the device moves in the given time. The formula typically used to determine the throughput T is,

$$T = BW \cdot \log_2\left(1 + \frac{SNR \cdot G}{N_0}\right) \quad (25)$$

where, G is Channel gain (with or without RIS), N_0 is Noise power spectral density.

4. SIMULATION RESULTS AND DISCUSSION

Table 2 displays the simulation parameters for various model networks. The graphs of IoT mMIMO DL NOMA devices illustrate the variations in capacity and SE, and SNR under different conditions. The outcomes are displayed before and following the implementation of RIS, which enhances the latency with device mobility, throughput, and coverage area of the network among the group of devices, while also tackling the difficulties posed by an abundance of IoT devices and resource-intensive 6G network applications. Fig. 3 flowchart shows the methodology process and the simulation steps required.

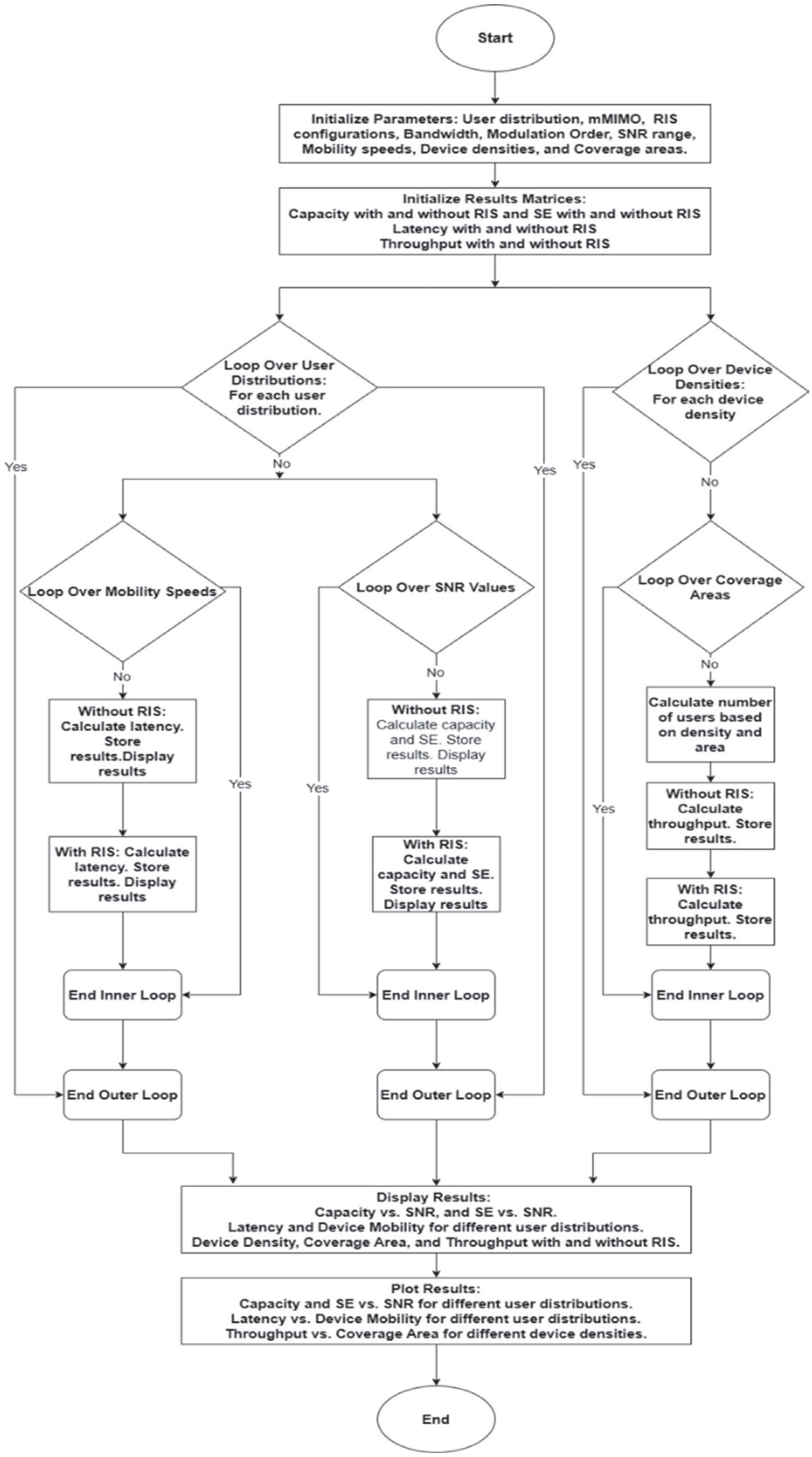

Fig. 3. Three types of IoT mMIMO DL NOMA cases with and without RIS systems are shown in a flow chart

In the 6G network, Fig. 4 illustrates the interaction between the capacity rate and SNR for four mMIMO DL NOMA IoT groups, both with and without the RIS method. The IoT devices own channels that exhibit variations in both distance and power distribution. A strong association existed between the capacity rate and the SNR. The group in the cluster with fewer devices (50 devices) supports the highest achievable capacity of 1.29 Mbps/Hz. The capacity rates for the second group with (100 devices), the third group with (150 devices), and the fourth group with (200 devices) were calculated to be 0.648, 0.432, and 0.324 Mbps/Hz, respectively. All four IoT groups saw capacity improvements of 5.84%, 5.81, 5.78, and 5.8% when using RIS, compared to their performance without RIS. This was confirmed at the SNR of 30 dB.

Table 2. Presents comprehensive information on the simulators employed for simulating various models

Parameter	Value
Devices Groups	50, 100, 150, and 200
Modulations	256 QAM
Path-loss exp.	4
BW	6 G Hz
Antennas No.	128x128 mMIMO
RIS	128x128
SNR	0 to 30 dB
Mobility Speed	(0-120) km/h
Coverage Areas	(100, 200, 300, 400) m2 or sqm

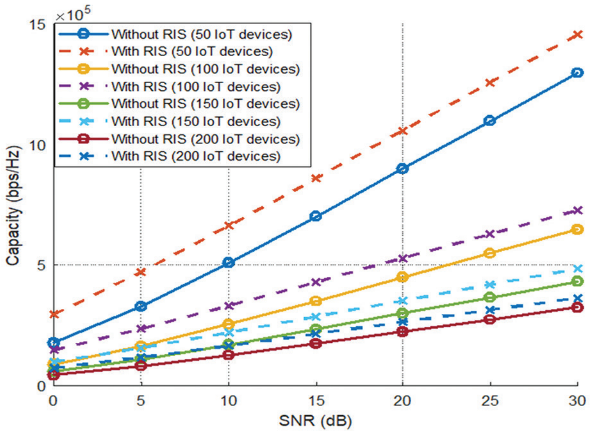

Fig. 4. Capacity rate vs. SNR for 4 groups in the IoT mMIMO DL NOMA network with and without RIS system

Within the 6G network, Fig. 5 depicts the correlation between the SE and SNR for four mMIMO DL NOMA IoT groups, both with and without the RIS architecture, and a strong correlation between SE and SNR was observed. The subgroup inside the cluster consisting of 50 devices allows for the maximum attainable SE of 0.21629 bps/Hz. The predicted SE rates for the second group consisting of 100 devices, the third group with 150 devices, and the fourth group consisting of 200 devices were determined to be 0.10815, 0.072097, and 0.054073 bps/Hz, respectively. All four IoT groups experienced SE enhancements of 5.759%, 5.755%, 5.753%, and 5.84%, respectively, when employing RIS, in comparison to their performance in the absence of RIS. This was verified at the SNR of 30 dB. The final result exceeded the results obtained according to references.

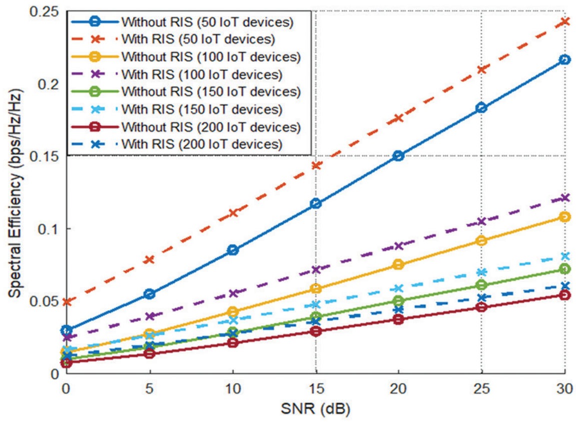

Fig. 5. SE against SNR for 4 groups in the IoT mMIMO DL NOMA network with and without RIS technique

Implementing RIS in the mMIMO system notably improves both the transmission capacity and the efficiency of spectrum utilization. The primary factor behind this enhancement is the improved effective channel gain offered by RIS, which amplifies the signal strength, hence generating more capacity and optimizing the utilization of the bandwidth. This improvement is especially noticeable at increased SNR levels and broader user dispersal, rendering RIS a valuable solution in IoT and 6G networks. The final result exceeded the results obtained according to references [48].

Fig. 6 illustrates the correlation between latency vs. device mobility with and without RIS for Different IoT Device Distributions for four mMIMO NOMA groups. The study focuses on a 6G network in different mobility scenarios: from 0 km/h to 120 km/h. During periods of slow movement or immobility, the channel conditions between the transmitter (such as BS) and the receiver (such as an IoT device) stay rather constant. The stability of the channel results in less fast fluctuations in both channel gains and signal quality, therefore enabling more consistent and dependable communication. By contrast, the channel conditions of faster-moving devices undergo rapid changes as a result of phenomena like as Doppler shift, multipath fading, and frequent handovers between various BS. Fluctuations in signal quality caused by these quick changes might result in increased delay, greater packet loss, and more frequent mistakes.

The subgroup inside the cluster, which has 50 devices, enables a minimum achievable latency of 2.44 milliseconds. The estimated latency rates for the second group, which included 100 devices, the third group, which included 150 devices, and the fourth group, which included 200 devices, were analyzed and found to be 1.72 ms, 1.48 ms, and 1.36 ms accordingly, at a velocity of 120 Km/h.

Implementing RIS resulted in latency rate improvements of 16.44%, 12.24%, 9.75%, and 8.1% for all four IoT groups, respectively.

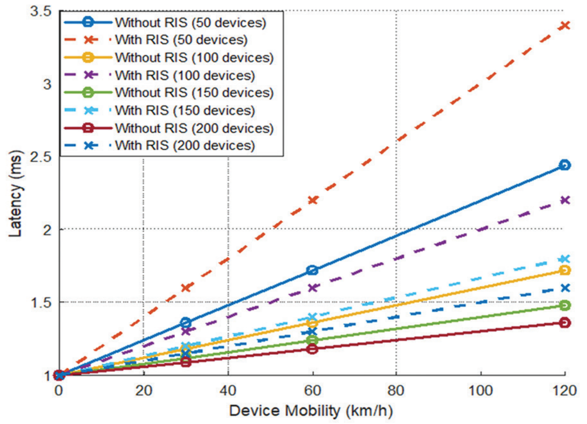

Fig. 6. Latency vs. Device Mobility with and without RIS for Different 4 groups IoT mMIMO DL NOMA Device Distributions

Fig. 7 depicts the relationship between Throughput and Coverage Area for four mMIMO NOMA groups, both with and without RIS, with varying device densities.

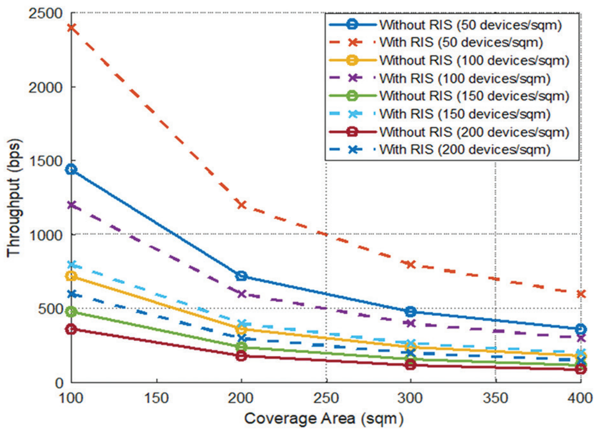

The study examines a 6G network under several Device Density scenarios, namely 100, 200, 300, and 400 square metres. Coefficient of inverse correlation between Throughput and coverage area. The subgroup inside the cluster, including 50 devices, allows for the maximum attainable throughput of 360 bps/Hz. The predicted throughput rates for the second group consisting of 100 devices, the third group with 150 devices, and the fourth group containing 200 devices were determined to be 180, 120, and 90 bps/Hz, respectively at the coverage area of 400 square meters (sqm). Each of the four IoT groups saw throughput improvements of 26%, 25.6%, 25.3%, and 25% correspondingly while using RIS. The augmented channel gains that RIS facilitates are primarily to blame for the increase and improvement in throughput. The RIS enhances signal propagation by dynamically regulating signal reflections, leading to improved connection quality and optimizing resource utilization, minimizing delay, and countering the effects of multipath fading. By adding NOMA, throughput is increased, making RIS-assisted NOMA a powerful method for fast communication in future 6G networks.

Fig. 7. Throughput vs. coverage area with and without RIS for different 4 groups IoT mMIMO DL NOMA device densities

5. CONCLUSIONS

This study provides a thorough evaluation of RIS technology in a 6G network environment, specifically within the mMIMO DL NOMA-enabled IoT system. The results show that the proposed approach is a promising solution for future 6G IoT networks, significantly improving capacity and SE, particularly in high-density areas. By integrating RIS with DL NOMA systems, the research highlights its ability to boost communication performance, especially in clustered user scenarios, making it essential for optimizing system performance and resource utilization in IoT networks. Additionally, RIS greatly reduces latency in NOMA systems, regardless of user distribution or mobility speeds, and improves communication efficiency. The latency model used provides key insights into the impact of RIS and mobility on system performance. Furthermore, RIS enhances data transfer rates, supporting increased device densities in various IoT environments, and the throughput model demonstrates its ability to optimize network architecture. In conclusion, RIS presents considerable benefits for improving network performance in 6G IoT systems. Future studies should explore its integration with advanced technologies like machine learning-based resource allocation and dynamic spectrum management to further enhance NOMA system performance in diverse IoT scenarios.

6. ACKNOWLEDGEMENT

The authors extended their appreciation to Taif University, Saudi Arabia, for supporting this work through project number (TU-DSPP-2024-132).

7. FUNDING

The research was funded by Taif University, Taif, Saudi Arabia (TU-DSPP-2024-132).

8. REFERENCES

[1] T. Qiu, N. Chen, K. Li, M. Atiquzzaman, W. Zhao, "How Can Heterogeneous Internet of Things Build Our Future: A Survey", IEEE Communications Surveys & Tutorials, Vol. 20, No. 3, 2018, pp. 2011-2027.

[2] B. U. Rehman, et al. "Joint power control and user grouping for uplink power domain non-orthogonal multiple access", International Journal of Distributed Sensor Networks, Vol. 17, No. 12, 2021.

[3] M. Hassan et al. "BER Improvement of Cooperative Spectrum Sharing of NOMA in 5G Network", Pro-

ceedings of the IEEE 3rd International Maghreb Meeting of the Conference on Sciences and Techniques of Automatic Control and Computer Engineering, Benghazi, Libya, 21-23 May 2023, pp. 647-652.

[4] G. Fortino, C. Savaglio, G. Spezzano, M. Zhou, "Internet of Things as System of Systems: A Review of Methodologies, Frameworks, Platforms, and Tools", IEEE Transactions on Systems, Man, and Cybernetics: Systems, Vol. 51, No. 1, 2021, pp. 223-236.

[5] Y. Al Mtawa, A. Haque, B. Bitar, "The Mammoth Internet: Are We Ready?", IEEE Access, Vol. 7, 2019, pp. 132894-132908.

[6] Y. Qian, D. Wu, W. Bao, P. Lorenz, "The Internet of Things for Smart Cities: Technologies and Applications", IEEE Network, Vol. 33, No. 2, 2019, pp. 4-5.

[7] N. N. Elmadina et al. "Performance of Power Allocation Under Priority User in CR-NOMA", Proceedings of the IEEE 3rd International Maghreb Meeting of the Conference on Sciences and Techniques of Automatic Control and Computer Engineering, Benghazi, Libya, 21-23 May 2023, pp. 618-622.

[8] L. U. Khan, I. Yaqoob, M. Imran, Z. Han, C. S. Hong, "6G Wireless Systems: A Vision, Architectural Elements, and Future Directions", IEEE Access, Vol. 8, 2020, pp. 147029-147044.

[9] B. Zheng, Q. Wu, R. Zhang, "Intelligent Reflecting Surface-Assisted Multiple Access With User Pairing: NOMA or OMA?", IEEE Communications Letters, Vol. 24, No. 4, 2020, pp. 753-757.

[10] F. Solano, S. Krause, C. Wöllgens, "An Internet-of-Things Enabled Smart System for Wastewater Monitoring", IEEE Access, Vol. 10, 2022, pp. 4666-4685.

[11] Y. Zhang et al. "Performance Analysis of CF-mMIMO-Aided SWIPT IoT Networks With Nonideal RF Response and Low-Resolution ADCs/DACs", IEEE Sensors Journal, Vol. 24, No. 3, 2024, pp. 3594-3607.

[12] M. Hassan et al. "NOMA Cooperative Spectrum Sharing Average Capacity Improvement in 5G Network", Proceedings of the IEEE 3rd International Maghreb Meeting of the Conference on Sciences and Techniques of Automatic Control and Computer Engineering, Benghazi, Libya, 21-23 May 2023, pp. 653-658.

[13] K. Senel, H. V. Cheng, E. Björnson, E. G. Larsson, "What Role can NOMA Play in Massive MIMO?", IEEE Journal of Selected Topics in Signal Processing, Vol. 13, No. 3, 2019, pp. 597-611.

[14] Y. Zhang, L. Xiao, T. Jiang, "Cloud-Based Cell-Free Massive MIMO Systems: Uplink Error Probability Analysis and Near-Optimal Detector Design", IEEE Transactions on Communications, Vol. 70, No. 2, 2022, pp. 797-809.

[15] Y. Zhang, B. Di, H. Zhang, J. Lin, Y. Li, L. Song, "Reconfigurable Intelligent Surface Aided Cell-Free MIMO Communications", IEEE Wireless Communications Letters, Vol. 10, No. 4, 2021, pp. 775-779.

[16] M. W. Akhtar, S. A. Hassan, S. Saleem, H. Jung, "STBC-Aided Cooperative NOMA With Timing Offsets, Imperfect Successive Interference Cancellation, and Imperfect Channel State Information", IEEE Transactions on Vehicular Technology, Vol. 69, No. 10, 2020, pp. 11712-11727.

[17] M. Hassan et al. "Capacity Enhancement Based on mMIMO for Cognitive Radio NOMA in Future 6G Networks", Proceedings of the IEEE 4th International Maghreb Meeting of the Conference on Sciences and Techniques of Automatic Control and Computer Engineering, Tripoli, Libya, 19-21 May 2024, pp. 387-392.

[18] J. Zuo, Y. Liu, Z. Ding, L. Song, H. V. Poor, "Joint Design for Simultaneously Transmitting and Reflecting (STAR) RIS Assisted NOMA Systems", IEEE Transactions on Wireless Communications, Vol. 22, No. 1, 2023, pp. 611-626.

[19] Z. Ding, R. Schober, H. V. Poor, "On the Impact of Phase Shifting Designs on IRS-NOMA", IEEE Wireless Communications Letters, Vol. 9, No. 10, 2020, pp. 1596-1600.

[20] R. Shafin, L. Liu, "Multi-Cell Multi-User Massive FD-MIMO: Downlink Precoding and Throughput Analysis", IEEE Transactions on Wireless Communications, Vol. 18, No. 1, 2019, pp. 487-502.

[21] Z. Chen, F. Sohrabi, W. Yu, "Multi-Cell Sparse Activity Detection for Massive Random Access: Massive MIMO Versus Cooperative MIMO", IEEE Transac-

tions on Wireless Communications, Vol. 18, No. 8, 2019, pp. 4060-4074.

[22] L. D. Nguyen, H. D. Tuan, T. Q. Duong, H. V. Poor, L. Hanzo, "Energy-Efficient Multi-Cell Massive MIMO Subject to Minimum User-Rate Constraints", IEEE Transactions on Communications, Vol. 69, No. 2, 2021, pp. 914-928.

[23] M. Amjad, L. Musavian, M. H. Rehmani, "Effective Capacity in Wireless Networks: A Comprehensive Survey", IEEE Communications Surveys & Tutorials, Vol. 21, No. 4, 2019, pp. 3007-3038.

[24] M. H. Babikir et al. "Optimization Efficiency of 5G MIMO Cooperative Spectrum Sharing NOMA Networks", Proceedings of the 9th International Conference on Mechatronics Engineering, Kuala Lumpur, Malaysia, 13-14 August 2024, pp. 183-187.

[25] S. Zhang, R. Zhang, "Intelligent Reflecting Surface Aided Multi-User Communication: Capacity Region and Deployment Strategy", IEEE Transactions on Communications, Vol. 69, No. 9, 2021, pp. 5790-5806.

[26] S. Ahmed, M. Z. Chowdhury, Y. M. Jang, "Energy-Efficient UAV-to-User Scheduling to Maximize Throughput in Wireless Networks", IEEE Access, Vol. 8, 2020, pp. 21215-21225.

[27] J. Li, X. Li, Y. Bi, J. Ma, "Energy-Efficient Joint Resource Allocation With Reconfigurable Intelligent Surfaces in Symbiotic Radio Networks", IEEE Transactions on Cognitive Communications and Networking, Vol. 8, No. 4, 2022, pp. 1816-1827.

[28] M. Hassan et al. "Modeling of NOMA-MIMO-Based Power Domain for 5G Network under Selective Rayleigh Fading Channels", Energies, Vol.15, 2022, p. 5668.

[29] P. Ramezani, Y. Zeng, A. Jamalipour, "Optimal Resource Allocation for Multiuser Internet of Things Network With Single Wireless-Powered Relay", IEEE Internet of Things Journal, Vol. 6, No. 2, 2019, pp. 3132-3142.

[30] K. Shafique, B. A. Khawaja, F. Sabir, S. Qazi, M. Mustaqim, "Internet of Things (IoT) for Next-Generation Smart Systems: A Review of Current Challenges, Future Trends and Prospects for Emerging 5G-IoT Scenarios", IEEE Access, Vol. 8, 2020, pp. 23022-23040.

[31] C. Pan et al. "Reconfigurable Intelligent Surfaces for 6G Systems: Principles, Applications, and Research Directions", IEEE Communications Magazine, Vol. 59, No. 6, 2021, pp. 14-20.

[32] Y. Liu et al. "Reconfigurable Intelligent Surfaces: Principles and Opportunities", IEEE Communications Surveys & Tutorials, Vol. 23, No. 3, 2021, pp. 1546-1577.

[33] R. Deshpande, M. V. Katwe, K. Singh, Z. Ding, "Resource Allocation Design for Spectral-Efficient URLLC Using RIS-Aided FD-NOMA System", IEEE Wireless Communications Letters, Vol. 12, No. 7, 2023, pp. 1209-1213.

[34] A. Khaleel, E. Basar, "A Novel NOMA Solution With RIS Partitioning", IEEE Journal of Selected Topics in Signal Processing, Vol. 16, No. 1, 2022, pp. 70-81.

[35] B. Zheng, C. You, R. Zhang, "Intelligent Reflecting Surface Assisted Multi-User OFDMA: Channel Estimation and Training Design", IEEE Transactions on Wireless Communications, Vol. 19, No. 12, 2020, pp. 8315-8329.

[36] Y. Cheng, K. H. Li, Y. Liu, K. C. The, H. Vincent Poor, "Downlink and Uplink Intelligent Reflecting Surface Aided Networks: NOMA and OMA", IEEE Transactions on Wireless Communications, Vol. 20, No. 6, 2021, pp. 3988-4000.

[37] T. Hou, Y. Liu, Z. Song, X. Sun, Y. Chen, "MIMO-NOMA Networks Relying on Reconfigurable Intelligent Surface: A Signal Cancellation-Based Design", IEEE Transactions on Communications, Vol. 68, No. 11, 2020, pp. 6932-6944.

[38] M. Mohammadi, H. Q. Ngo, M. Matthaiou, "Phase-Shift and Transmit Power Optimization for RIS-Aided Massive MIMO SWIPT IoT Networks", IEEE Transactions on Communications, 2024. (in press)

[39] B. Ur Rehman et al. "Uplink power control scheme for spectral efficiency maximization in NOMA systems", Alexandria Engineering Journal, Vol. 64, 2023, pp. 667-677.

[40] N. Elmadina et al. "Downlink Power Allocation for CR-NOMA-Based Femtocell D2D Using Greedy Asynchronous Distributed Interference Avoidance Algorithm", Computers, Vol. 12, 2023, p. 158.

[41] T. Guo et al. "A Hybrid Indoor Positioning Algorithm for Cellular and Wi-Fi Networks", Arabian

Journal for Science and Engineering, Vol. 47, 2022, pp. 2909–2923.

[42] J. Fei, S. Li, "Adaptive Fractional High Order Sliding Mode Fuzzy Control of Active Power Filter", Proceedings of the Joint 10th International Conference on Soft Computing and Intelligent Systems and 19th International Symposium on Advanced Intelligent Systems, Toyama, Japan, 5-8 December 2018, pp. 576-580.

[43] H. Liu, G. Li, X. Li, Y. Liu, G. Huang, Z. Ding, "Effective Capacity Analysis of STAR-RIS-Assisted NOMA Networks", IEEE Wireless Communications Letters, Vol. 11, No. 9, 2022, pp. 1930-1934.

[44] E. Basar, I. Yildirim, "Reconfigurable Intelligent Surfaces for Future Wireless Networks: A Channel Modeling Perspective", IEEE Wireless Communications, Vol. 28, No. 3, 2021, pp. 108-114.

[45] S. Jia, X. Yuan, Y.-C. Liang, "Reconfigurable Intelligent Surfaces for Energy Efficiency in D2D Communication Network", IEEE Wireless Communications Letters, Vol. 10, No. 3, 2021, pp. 683-687.

[46] M. Hassan, M. Singh, K. Hamid, R. Saeed, M. Abdelhaq, R. Alsaqour, N. Odeh, "Enhancing NOMA's Spectrum Efficiency in a 5G Network through Cooperative Spectrum Sharing", Electronics, Vol. 12, 2023, p. 815.

[47] M. Hassan et al. "Design of Power Location Coefficient System for 6G Downlink Cooperative NOMA Network", Energies, Vol. 15, 2022, p. 6996.

[48] A. BANON, Fayez W. Zaki, M. M. Ashour, "The effect of quantized ETF, grouping, and power allocation on non-orthogonal multiple accesses for wireless communication networks", International Journal of Electrical and Computer Engineering Systems, Vol. 13, No. 8, 2022, pp. 681-693.